Remote Sensing in Earth Systems Sciences (2026) 9:28
https://doi.org/10.1007/s41976-026-00278-z

RESEARCH

Validation of Satellite-based and Gridded Precipitation Products for Gap-filling in Precipitation Series in the Eastern Amazon

Giselle Nerino Brito de Souza[1] · Julie Andrews de França e Silva[2] · Kaleb Lima Ribeiro[2] · Leonardo Ramos de Oliveira[3] · Paulo Ricardo Teixeira da Silva[4] · Débora Cristina Castellani[5] · Júlio Sílvio de Sousa Bueno Filho[6] · Alailson Venceslau Santiago[7] · Steel Silva Vasconcelos[8] · Wenceslau Geraldes Teixeira[9] · Alessandro Carioca de Araújo[7]

Received: 30 September 2025 / Revised: 7 March 2026 / Accepted: 22 March 2026

Abstract

Accurate precipitation measurement is essential for climate, hydrological, and agronomic studies. However, in regions such as the Amazon, the scarcity of rain gauges and frequent gaps in historical series pose a significant challenge for long-term analyses. This study evaluated the performance of satellite and gridded precipitation estimates for gap-filling daily rainfall data recorded between 2019 and 2024. The observed dataset was obtained from a micrometeorological tower installed in an oil palm-based Agroforestry System (AFS) in the Eastern Amazon. The evaluation employed widely recognized statistical metrics, such as the coefficient of determination (R^2), root mean square error (RMSE), mean absolute error (MAE), percent bias (PBIAS), Nash-Sutcliffe efficiency (NSE), and Willmott's index of agreement (d). Additionally, cumulative precipitation curves from different databases were compared with the observed series to identify over- or underestimation trends. The results showed that, among the tested databases, NASA Power (NP) exhibited the best performance in terms of consistency and lower bias, making it the most suitable for filling gaps in the observed series. The analyses highlighted the importance of a careful selection of alternative databases to ensure data continuity and quality in remote tropical regions, an essential aspect for hydrological modeling studies.

Keywords rainfall gap-filling · satellite precipitation · meteorological tower · agroforestry system

✉ Giselle Nerino Brito de Souza
gisellenerino@gmail.com

Julie Andrews de França e Silva
julieandrewsfranca@gmail.com

Kaleb Lima Ribeiro
kaleblimar@gmail.com

Leonardo Ramos de Oliveira
lrdo87@gmail.com

Paulo Ricardo Teixeira da Silva
paulo.ricardo.teixeira@gmail.com

Débora Cristina Castellani
deboracastellani@natura.net

Júlio Sílvio de Sousa Bueno Filho
jssbueno@ufla.br

Alailson Venceslau Santiago
alailson.santiago@embrapa.com

Steel Silva Vasconcelos
steel.vasconcelos@embrapa.br

Wenceslau Geraldes Teixeira
wenceslau.teixeira@embrapa.br

Alessandro Carioca de Araújo
alessandro.araujo@embrapa.br

[1] Federal Rural University of Amazon (UFRA), Belém, Pará, Brazil

[2] The Large-Scale Biosphere–Atmosphere Research Program in the Amazon (LBA), National Institute for Amazonian Research (INPA), Belém, Pará, Brazil

[3] National Institute for Amazonian Research (INPA), Manaus, Amazonas, Brazil

[4] The Large-Scale Biosphere–Atmosphere Research Program in the Amazon (LBA), Manaus, Amazonas, Brazil

[5] Natura Innovation and Product Technology Ltd, Cajamar, São Paulo, Brazil

[6] Federal University of Lavras, Lavras, Minas Gerais, Brazil

[7] Brazilian Agricultural Research Corporation, Belém, Pará, Brazil

[8] Brazilian Agricultural Research Corporation, Colombo, Paraná, Brazil

[9] Brazilian Agricultural Research Corporation, Rio de Janeiro, Rio de Janeiro, Brazil

Published online: 30 March 2026

1 Introduction

The Amazon plays a fundamental role in regulating the regional and global hydrological cycle. Rainfall variability in tropical ecosystems directly influences all components of the water balance [29, 40], triggering multi-year cycles of precipitation excess and scarcity that manifest in different parts of the Amazon region [21, 23].

The seasonality and distribution of rainfall in the Amazon are directly influenced by large-scale climate systems, including the Intertropical Convergence Zone (ITCZ), the South Atlantic Convergence Zone (SACZ), and the El Niño-Southern Oscillation (ENSO) phenomenon (Fisch et al., 1998; [11, 37, 41, 45]). Extreme climatic events, such as those caused by El Niño, tend to accentuate the occurrence of prolonged droughts, affecting important ecosystem processes, including soil water storage and, consequently, agricultural productivity (17, 20). Such events have become more frequent and intense in recent decades, reinforcing the importance of understanding and monitoring rainfall in the region [4, 23].

However, the sparse distribution of rain gauges and recurrent gaps in historical series compromise accurate precipitation analysis, especially in remote and hard-to-access regions like the Amazon [40]. Added to the spatial and temporal variability of precipitation, this is a critical factor for hydrological monitoring and modeling, particularly in areas with limited data collection infrastructure. This methodological gap is even more relevant in productive systems such as agroforestry, which have been expanding in the Eastern Amazon but remains understudied from a hydrometeorological perspective.

Considering this context, in addition to data from meteorological stations, such as those from the National Institute of Meteorology (INMET), and reanalysis products, such as the Xavier product, remote sensing data are also widely used, including the Climate Hazards Group InfraRed Precipitation with Station data (CHIRPS), the Global Precipitation Measurement (GPM), and NASA's Prediction of Worldwide Energy Resources (POWER/NP). These products complement observed data and allow for more robust analyses of precipitation trends and patterns at expanded temporal and spatial scales (25, 31 , 47).

Studies on water dynamics in productive systems depend on complete and consistent rainfall series, since precipitation is generally the main input variable in water balance models and soil flow simulations [9, 19, 48]. The presence of gaps in these series compromises the quality of the results and, in many cases, makes continued analysis unfeasible. Thus, rainfall gap-filling constitutes an indispensable methodological step for environmental modeling [22], agricultural management, and water planning [35, 36]. Despite the growing availability of satellite and reanalysis data, there is still a scarcity of studies that systematically evaluate the performance of these products in filling gaps in observed series, especially in agricultural production areas of the Amazon.

Given this, the objective of the present study was to evaluate the performance of rainfall estimates from conventional and satellite-based sources for gap-filling daily rainfall data recorded by a micrometeorological observation tower installed in an agroforestry system in the Eastern Amazon.

2 Materials and Methods

2.1 Study Area

The study was conducted on a rural property located in the municipality of Tomé-Açu, Pará State, Brazil (2∘24′15″S; 48∘14′53.3″W) (Fig. 1). The region features a hot and humid tropical climate, classified as Am according to Köppen, with an approximate annual mean temperature of 26.4 °C and an annual mean precipitation of 2,300 mm [1].

The local relief is gently undulating, composed of low flattened plateaus, terraces, and floodplains, with altitudes ranging from 14 m to 96 m. The predominant soil is Dystrophic Yellow Latosol (Oxisol), typical of the Amazon region [32]. The original vegetation corresponds to Dense Ombrophilous Forest, which is currently significantly altered due to anthropogenic use. The present landscape is a mosaic of urban areas, secondary forests, and agricultural activities, including Agroforestry Systems (AFS).

In March 2008, an AFS was established in an area previously occupied by an abandoned orchard for 11 years, designated as Demonstration Unit 1 (UD-1). The system exhibits high species diversity, composed of double rows of oil palm (*Elaeis guineensis* Jacq.), spaced at 9.0 × 9.0 × 9.0 m, interspersed with 21-m wide strips containing agricultural and forest species. Currently, the study area consists mainly of intercropped oil palm, açaí (*Euterpe oleracea* Mart.), cocoa (*Theobroma cacao* L.), and forest species. The complete list of species composing the AFS can be found in Barros et al., 2025 [3].

2.2 Data Collection and Instrumentation

In the study area, a 23 m-high micrometeorological observation tower was installed in 2019. The tower is equipped with instruments that perform continuous, low-frequency measurements of micrometeorological variables, both below and above the AFS canopy (Fig. 2a).

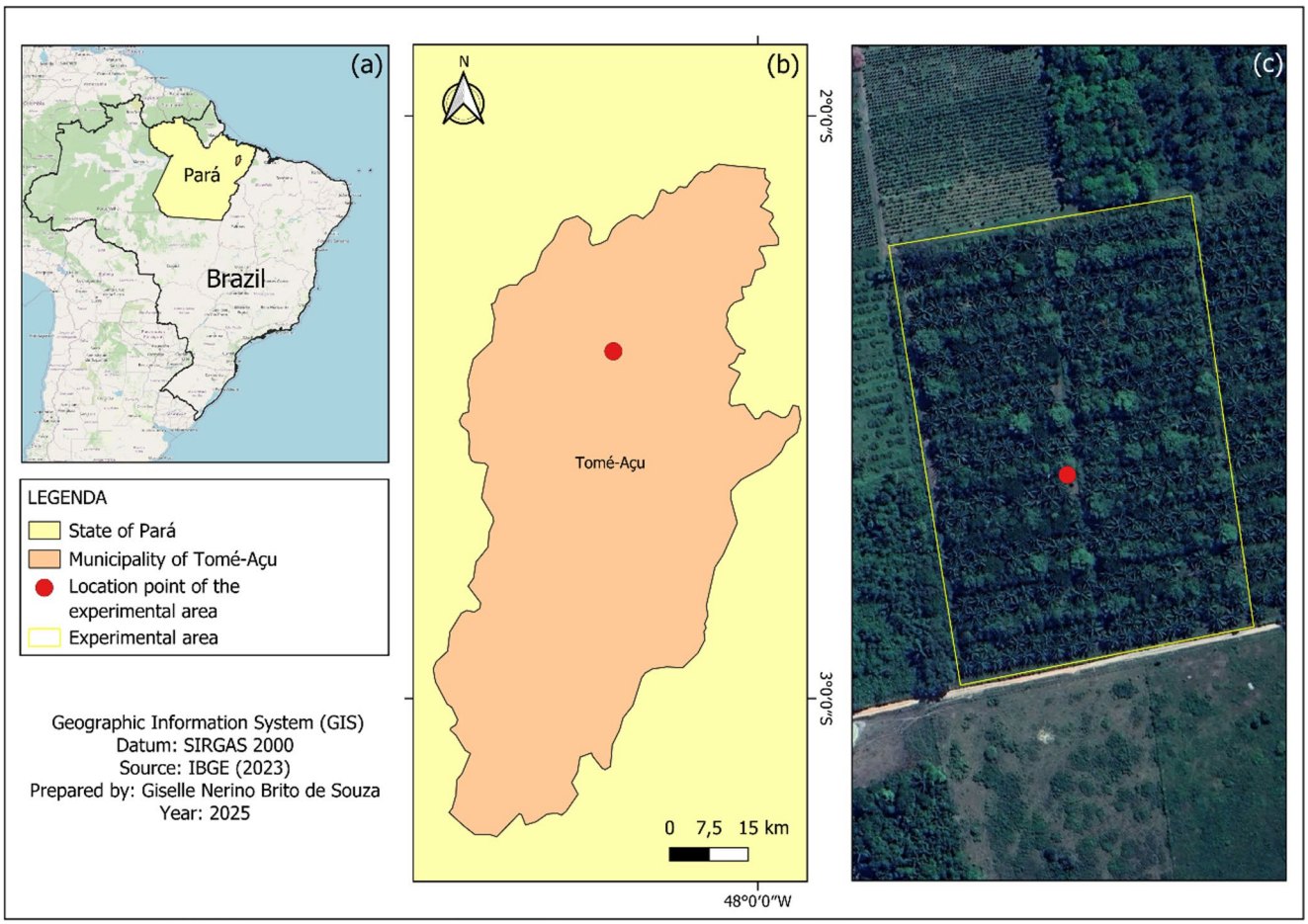

Fig. 1 Geographical location of the experimental area. (**a**) Position of Pará State within the Brazilian territory; (**b**) Municipality of Tomé-Açu, with the red dot indicating the location of the experimental area; (**c**) Satellite image of the experimental area, outlined in yellow, where the red dot represents the location of the installed micrometeorological tower

Measurements were recorded by an electronic micrologger (CR1000, Campbell Scientific, Inc., USA), which samples values every 60 s. Precipitation data were calculated by summing the rainfall events and recorded at a 30-minute temporal resolution. Data were stored in both the equipment's internal memory and high-performance memory cards (CFM2G, Campbell Scientific, Inc., Logan, UT, USA). These cards were replaced monthly during field visits, and data could also be accessed via telemetry. After collection, the data underwent assessment and quality control, excluding values outside possible physical limits, following microclimatic studies and the protocol adopted by the Large-Scale Biosphere-Atmosphere Experiment in Amazonia (LBA).

The rain gauge used in this study is a tipping-bucket type with a precision of 0.198 mm (PluviDB, Dual Base, Brazil), installed on the tower at a height of 21 m above the ground (Fig. 2b). This instrument is widely used in automatic monitoring stations for climatological and hydro-environmental parameters due to its simple, easily understood mechanism and relatively low manufacturing costs [15, 33]. Its operation is based on a double-tipping system: rainwater is collected by a funnel (Fig. 3a) and directed to a small chamber containing two buckets (Fig. 3b).

Each time one of the buckets accumulates a specific volume of water, equivalent to 0.198 mm of precipitation, an automatic tipping occurs, emptying the full compartment and positioning the other for the next collection. This movement triggers a magnetic reed switch, generating an electrical signal sent to the data acquisition system, allowing for the continuous recording of accumulated precipitation [6].

To ensure the consistency of the time series, we identified the need to perform gap-filling for days where more than 20% of the data were missing, which corresponds to more than 288 min per day of missing or invalid data. In total, 209 days without precipitation data were identified.

The time series consisted of 2,141 days, of which 1,932 days (approximately 90.3% of the series) presented valid observed data. For this period, the average daily precipitation recorded at the TSAF tower was 6.5 mm day^{-1}. This

Fig. 2 Micrometeorological observation tower in the municipality of Tomé-Açu, Pará (**a**); Location of the tipping bucket rain gauge. (**b**) Source: Giselle Nerino (**a**); Leonardo Ramos (**b**)

Fig. 3 Funnel (**a**) and buckets (**b**) of the DualBase PluviDB rain gauge instrument installed on the tower [7]

average value served as a baseline for evaluating the performance of the gap-filling models, allowing us to verify if the regression-corrected estimates outperformed the simple local climatology.

The 209 days identified for gap-filling were intermittently distributed throughout the study period, from February 21, 2019, to December 31, 2024. These gaps were primarily characterized by short-term isolated events (1 to 2 days) or intermittent sequences (typically 3 to 7 days). Isolated gaps were predominantly associated with routine maintenance procedures, such as cleaning the collection funnel or recording spurious tipping during technical inspections. The short-to-medium-term sequences were mainly attributed to system operation interruptions caused by power failures, technical issues, or physical obstructions in the tipping mechanism, such as the accumulation of leaves and insects. Since these gaps were dispersed rather than concentrated in a single large block, the overall seasonal pattern of the historical series remained intact, supporting the application of daily-scale reconstruction methods.

This criterion was adopted based on the quality control protocols established by the LBA. The 288-minute limit (20% of the 1,440 min in a day) serves as a safeguard to ensure that the calculated daily precipitation totals remain representative of actual weather conditions. In the Amazonian context, where high-intensity convective rains frequently occur in brief intervals, the loss of more than 20% of daily records significantly increases the risk of missing a major rain event, thus compromising the integrity of the daily total. This approach allowed for the rigorous identification of the 209 days requiring reconstruction to maintain long-term series consistency.

2.3 Precipitation Data Sources and Processing

Tests involving the creation of artificial gaps for cross-validation were performed. However, these preliminary tests did not provide a reliable basis for selecting a gap-filling source and often obscured the products' ability to capture broader seasonal trends due to the extreme spatio-temporal variability of daily precipitation in the Eastern Amazon, which is characterized by localized convective events.

To complete the precipitation series, five databases were chosen, selected based on their spatial coverage characteristics, temporal resolution, and availability for the study site. The databases include satellite products as well as data from meteorological stations and gridded reanalyses, reflecting different methodologies for data acquisition and interpolation [12, 8].

A point-to-pixel comparison approach was adopted. Precipitation values were extracted specifically from the grid cell (pixel) of each product that overlapped the geographic coordinates of the micrometeorological tower (2° 24' 15" S; 48°14' 53.3" W). No spatial homogenization (resampling of all products to a common grid) was performed, aiming to evaluate the native accuracy of each dataset in representing local precipitation. This approach avoids interpolation artifacts that could bias validation results, providing a realistic assessment of the performance of these 'ready-to-use' products for local gap-filling.

The selection of a single pixel, rather than a spatial average of neighboring pixels, aimed to preserve the native variability and error structures of each product at a local scale. This approach avoids the smoothing of intense, short-duration convective events, a prominent characteristic of rainfall in the Eastern Amazon, ensuring that the validation metrics accurately reflect the potential of each source to represent the specific conditions of the agroforestry system. The following datasets were used:

- Global Precipitation Measurement (GPM): Precipitation estimates from the GPM mission, developed in cooperation between the National Aeronautics and Space Administration (NASA) and the Japan Aerospace Exploration Agency (JAXA), were obtained through the IMERG (Integrated Multi-satellitE Retrievals for GPM) version 6 product. This product integrates data from active and passive sensors, such as the GPM Microwave Imager (GMI) and the Dual-frequency Precipitation Radar (DPR), which have been operational since 2014. The selection of IMERG v6 is justified by its high spatial resolution (0.1°, approximately 10 km) and high temporal frequency (30 min) [14]. For this analysis, data spanning the period from February 21, 2019, to June 3, 2024, were used.
- NASA Prediction Of Worldwide Energy Resources (NASA POWER): NASA project that provides satellite-derived meteorological data with near-global coverage since 1981. The data are organized in geographical grids of 0.5° latitude by 0.625° longitude (approximately 55.5 × 70 km) and are widely used for energy and climate studies [38]; NASA Power, [28]. The period of collected data spanned from February 21, 2019, to December 31, 2024.
- Climate Hazards Group InfraRed Precipitation with Station data (CHIRPS): It combines satellite data and rain gauges, with time series dating back to 1981, a spatial resolution of 0.05° (approximately 5 km), and daily frequency. It is recognized as an important database for climate studies in tropical and developing regions [13]. The period of collected data spanned from February 21, 2019, to December 30, 2024.
- Brazilian National Institute of Meteorology (INMET): INMET provides real-time observational data and historical series from an extensive network of automatic weather stations distributed throughout the Brazilian territory. Precipitation measurements are performed by automatic rain gauges, with records on hourly and daily bases, following standardized technical criteria for climate monitoring [16]. In the municipality of Tomé-Açu, the weather station used in this study (code A213) is located approximately 25 km from the micrometeorological observation tower installed in the agroforestry system (AFS). Data with hourly frequency were used and aggregated to a daily scale for the period from February 21, 2019, to December 30, 2024. However, the series presented missing data in the following intervals: April 20, 2019; from December 14, 2021, to June 21, 2023; and from September 19 to 27, 2024.
- Xavier: Database composed of daily and monthly precipitation estimates, organized in a spatial grid of 0.25° x 0.25°. The values were obtained through the interpolation of rain gauge station data, using methods such as Arithmetic Mean, Natural Neighbor, Inverse Distance Weighting (IDW), and Ordinary Kriging [44]. The period of collected data spanned from February 21, 2019, to March 20, 2024.

Precipitation data were organized into spreadsheets with a daily temporal resolution (mm/day). Statistical and graphical analyses were performed using a routine in the R programming language, utilizing codes developed to automate the processes and ensure the reproducibility of the data treatment and comparison stages. To evaluate the capacity of the different databases to fill the gaps in the precipitation series, simple linear regression analyses were performed between the data measured by the AFS tower and the data estimated by each external source, aiming to verify the degree of linear association between the series.

Initially, linear regression equations with a free intercept were fitted, allowing for the evaluation of the coefficient of determination (R^2) and the slope of the line for each database. However, considering that null precipitation should correspond to the absence of rain in both observed and estimated data, it was also decided to fit the equations with the intercept forced through the origin (zero).

The choice to use regression equations forced through the origin for the final reconstruction was dictated by the need for physical consistency in the precipitation time series. In a free-intercept model ($y = ax + b$), the presence of a non-zero constant (b) would result in the estimation of 'spurious rain' on days when the external satellite or gridded product recorded no precipitation. By forcing the intercept to zero, the model ensures that $y = 0$ when $x = 0$, thereby preserving the frequency of dry days in the filled series. In this context, the slope of the line (a) functions as a scaling factor that adjusts the magnitude of the external estimates to better align with the local intensity recorded at the tower site. This adjustment consistently improved the statistical fit and provided a more realistic representation of daily precipitation totals for the 209 missing days.

Based on these fitted equations, a new column of rainfall estimates was generated for each source, using exclusively

Table 1 Statistical techniques used for model performance evaluation

Statistical techniques	Description	Equation
Coefficient of Determination (R^2)	Association between observed and estimated values.	$R^2 = 1 - \frac{SSE}{SST}$
Root Mean Square Error (RMSE)	Average magnitude of the errors between observed and estimated values.	$\mathrm{RMSE} = \sqrt{\frac{1}{n}\Sigma(O_i - E_i)^2}$
Mean Absolute Error (MAE)	Mean of the absolute differences between observed and estimated values.	$MAE = \frac{1}{n}\Sigma\,(E_i - O_i)$
Percent Bias (PBIAS)	Indicates the tendency for overestimation or underestimation.	$\mathrm{PBIAS} = \frac{100 \times \Sigma E_i - \Sigma O_i}{\Sigma O_i}$
Nash–Sutcliffe Efficiency (NSE)	Efficiency of the estimates relative to the observed mean.	$\mathrm{NSE} = 1 - \frac{\Sigma(O_i - E_i)^2}{\Sigma(O_i - \overline{O_i})^2}$
Willmott's Index of Agreement (d)	Degree of agreement between observed and estimated values.	$d = 1 - \frac{\Sigma(E_i - O_i)^2}{\Sigma(E_i - \overline{O_i}) + (O_i - \overline{O_i})^2}$

SSE: Sum of Squared Errors (difference between observed and estimated values); SST: Total Sum of Squares (difference between observed values and the observed mean). Oi: observed values (SAF); Ei: estimated values (alternative sources); $\bar{O}$: mean of the observed values (SAF); n: number of observations

the slope coefficient multiplied by the daily precipitation value of the respective external base. This procedure was applied to all days with gaps in the tower series, filling the 209 missing days consistently with the statistical behavior identified for each data source.

Direct correlation between the complete series was used as a preliminary step to verify the alignment between the bases. However, given the low explanatory power of daily R^2 in tropical regions, it was decided to apply direct gap-filling methods and subsequently evaluate the performance of these techniques with specific statistical metrics, considering only the days originally missing from the tower series.

Although there were variations in the total temporal coverage period among the bases, validation and gap-filling were performed using only the consistent overlapping data intervals. Thus, the statistical representativeness of the correlation and performance analyses was preserved, ensuring the integrity of the reconstructed series for the AFS [18, 27, 34, 43].

The indices selected to evaluate the performance of the precipitation data estimates were the coefficient of determination (R^2), the Root Mean Square Error (RMSE), the Mean Absolute Error (MAE), the Percent Bias (PBIAS), the Nash-Sutcliffe Efficiency (NSE), and Willmott's index of agreement (d). The R^2 expresses the degree of linear correlation between estimated and observed values, while the RMSE quantifies the average magnitude of the errors, being sensitive to large discrepancies. The MAE represents the average of the absolute differences between observed and estimated values, being useful for interpreting the average error without considering its direction. The PBIAS allows for the identification of the systematic tendency for overestimation or underestimation of the estimates relative to the observed data. Furthermore, the NSE provides a measure of the overall predictive performance of the base, comparing it with the simple mean of the observed data as an estimate. Finally, Willmott's index of agreement (d) evaluates the proximity between estimated and observed values, ranging from 0 (no agreement) to 1 (perfect agreement), and is widely used to validate environmental and hydrological models [27, 43].

Descriptions and equations for each of the statistical indices are provided in Table 1. These statistical indicators allowed for the measurement of different aspects of the quality of the estimated data relative to the observed data, considering dispersion, bias, and efficiency. The combination of these parameters enables a more accurate assessment of which dataset exhibits the best performance for gap-filling in precipitation time series [46].

3 Results and Discussion

3.1 Comparative Assessment Between Observed and Estimated Data

To evaluate the performance of the different reconstruction models and assist in selecting the most suitable source for gap-filling, a descriptive analysis of the estimated data corresponding to the 209 missing days was first performed (Table 2). The NASA Power reconstruction, using the free-intercept model, presented the highest total accumulated precipitation (1,493.76 mm). These reconstructions were compared to the local historical variability to ensure the statistical integrity of the final series.

The NASA Power base presented the highest total accumulated precipitation over the analyzed period (1,493.76 mm), while the lowest total was estimated by the INMET base with zero-intercept regression (696.54 mm). In terms of daily average rainfall, the highest estimate was obtained by the NP base with a free intercept (7.15 mm), and the lowest by the INMET base (3.33 mm). The highest standard deviation was identified in the GPM base (8.20 mm), reflecting greater variability in the daily precipitation estimates.

The analysis of maximum daily values, which reflect the intensity of extreme events, showed that the GPM base (with zero intercept) presented the highest value

Table 2 Descriptive statistics of the daily precipitation reconstruction (mm/day) for the 209-day gaps, including total accumulation, mean, standard deviation, extreme values, and R^2 relative to the observed data

Reconstruction Model	Regression Type	Coefficient of Determination (R^2)	Total Rainfall (mm)	Min. (mm)	Max. (mm)	Mean (mm)	Standard Deviation
Nasa Power	Free Intercept (y = 0.6537x + 1.9084)	0.20	1493.76	1.91	39.82	7.15	5.94
Nasa Power	Zero Intercept (y = 0.7694x)	0.38	1288.69	0	44.63	6.17	6.99
GPM	Free Intercept (y = 0.2732x + 2.9869)	0.26	1360.95	2.99	70.49	6.51	6.73
GPM	Zero Intercept (y = 0.3329x)	0.41	897.67	0	82.26	4.3	8.2
CHIRPS	Free Intercept (y = 0.4733x + 3.0538)	0.16	1310.05	3.05	25.29	6.27	4.2
CHIRPS	Zero Intercept (y = 0.6164x)	0.33	874.92	0	28.96	4.19	5.47
Xavier	Free Intercept (y = 0.4167x + 3.3781)	0.14	1440.84	3.38	25.96	6.89	4.25
Xavier	Zero Intercept (y = 0.571x)	0.33	1006.91	0	30.94	4.82	5.83
Inmet	Free Intercept (y = 0.5235x + 3.5592)	0.20	1299.73	3.56	51.51	6.22	5.4
Inmet	Zero Intercept (y = 0.656x)	0.31	696.54	0	60.09	3.33	6.76

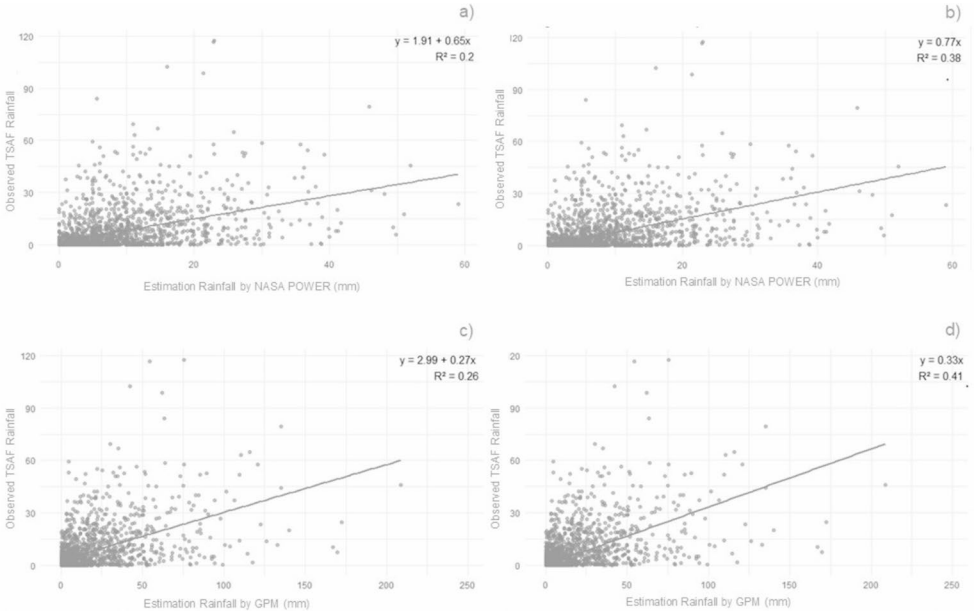

Fig. 4 Linear fits between observed and estimated data by the NASA POWER and GPM datasets, using regression models with a free intercept (**a** and **c**) and forced through the origin (**b** and **d**), over the study period. The graphs illustrate the performance of the datasets that yielded the best Coefficients of Determination (R^2), highlighting their potential for precipitation data gap-filling

(82.26 mm), while the lowest was recorded by the CHIRPS base (25.29 mm), evidencing the more conservative nature of the estimates from this source.

Regarding statistical performance, the coefficients of determination (R^2) indicated that the GPM base, with regression forced through the origin (zero intercept), achieved the best linear fit relative to the observed data, with $R^2 = 0.41$. This was followed by the NASA Power base with $R^2 = 0.38$. These results suggest that these two bases exhibit greater adherence to the data recorded at the tower's automatic station and, therefore, possess higher potential for use in gap-filling the precipitation time series (Fig. 4).

Additionally, a comparative analysis was performed between the original observed series ($n = 1{,}932$ days) and the final reconstructed series ($n = 2{,}141$ days). The results presented in Table 3 demonstrate that the daily mean remained around 6.5 mm for the datasets used, with the

Table 3 Comparative descriptive statistics between the measured precipitation series and the series generated by the different processing methods and databases

TSAF	Initial data	Regression Estimate	Reconstructed series
	6.5		
NP	7.12	5.48	6.47
GPM	14.81	4.3	6.51
CHIRPS	7.24	4.19	6.48
Xavier	8.41	4.82	6.54
INMET	5.04	3.33	6.48

Initial Data: For TSAF, this refers to the data observed in situ by the tower's micrometeorological sensor, corresponding to the effective operation period (1,932 days), including the original gaps. Regression-based Estimate: Refers to the values calculated for the total period (2,141 days) through the application of linear regression equations (with zero intercept) on the data from external sources. Reconstructed Series (Final): Refers to the final consolidated product, composed of the data measured from the tower, with the 209-day gaps filled by the Regression-based Estimates.

NASA POWER (NP) regression estimate showing the closest proximity to the original TSAF tower mean, reinforcing its consistency.

These results confirm that the insertion of 9.7% estimated data did not distort the local climatology, maintaining the robustness of the reconstruction despite the inherent biases of satellite and gridded products in the Amazon. Therefore, it is demonstrated that the regression methodology was statistically satisfactory for gap-filling without introducing significant distortions to the climatological characteristics of the TSAF tower database.

3.2 Statistical Performance Indicators of the Datasets for Gap-Filling

The performance of the different datasets for filling daily precipitation gaps in the observed data is presented in Table 4.

To verify if the gap-filling process compromised the homogeneity of the original time series, a comparative evaluation of descriptive statistics was performed before and after the inclusion of the 209 reconstructed days. The original TSAF series and the final series with filled gaps showed high consistency in fundamental parameters: the daily mean remained with a deviation of less than 5%, and the proportion of dry days was preserved due to the zero-intercept regression approach. Furthermore, the standard deviation and daily maximums of the filled data aligned with the local historical variability, indicating that the use of NASA Power for reconstruction did not introduce artificial trends or attenuate the magnitude of seasonal precipitation peaks. This statistical stability confirms that the final dataset is suitable for long-term hydrological modeling and water balance studies in the agroforestry system.

The coefficient of determination (R^2) ranged from 0.31 (INMET) to 0.41 (GPM), values that reflect limited linear correlation between the observed and estimated series. This performance is expected given the high spatio-temporal variability of precipitation on a daily scale, a prominent characteristic of the Amazon region, where short-duration convective events are frequent and difficult to represent by spatial databases. Previous studies reinforce that, in humid tropical regions, evaluation at more aggregated temporal scales tends to substantially improve statistical fit. Alves and Victoria, 2020 [2] highlight that utilizing ten-day or monthly series smooths the variability of extreme events, resulting in higher correlation values. Similarly, Tan et al., 2017 [39], when evaluating the GPM product, also observed that statistical performance improves considerably when precipitation is analyzed in broader time windows. Nevertheless, in the present study, the obtained linear correlation was sufficient to allow the adjustment of regression equations forced through the origin as a strategy to reduce potential biases. From these equations, corrected precipitation estimates were generated, which supported the filling of the 209 days with gaps in the tower series.

Table 4 Statistical indicators between observed data (AFS tower) and data estimated by different datasets

Indicador	GPM	NP	CHIRPS	INMET	XAVIER
R^2	0,41	0,38	0,33	0,31	0,33
RMSE (mm)	10,86	10,64	11,08	11,15	11,12
NSE	0,22	0,19	0,12	0,13	0,09
PBIAS (%)	-29	-17	-30	-47	-30
MAE (mm)	5,62	5,68	5,72	5,11	6,08
Índice d	0,65	0,58	0,55	0,60	0,54

The RMSE ranged between 10.64 mm (NP) and 11.15 mm (INMET), with this indicator being adopted as the primary comparison criterion as it reflects the dispersion of errors relative to observed values. The NP base presented the lowest RMSE, evidencing higher overall accuracy for gap-filling, while INMET recorded the highest value, indicating greater variability in the errors associated with its estimates.

The MAE ranged from 5.11 mm (INMET) to 6.08 mm (Xavier), indicating moderate differences in the average magnitude of absolute errors among the evaluated bases. The lower value observed for INMET suggests that, on average, this base's estimates were slightly closer to the observed values. However, this result should be interpreted alongside the other indicators, since the MAE, by not weighting the magnitude of extreme errors, may underestimate situations where large individual discrepancies occur [43]. The other bases showed similar performance, with values near 5.6 to 5.7 mm, reflecting general consistency in daily estimates.

The Nash-Sutcliffe Efficiency (NSE) coefficient presented positive values for all databases, ranging from 0.09 (Xavier) to 0.22 (GPM). Statistical indices demonstrate that, despite the inherent limitations of satellite and gridded products in reproducing all daily extreme events, the corrected estimates exhibit superior performance compared to using the climatological mean of the observed series (6.5 mm day^{-1}) as a gap-filling strategy. While applying a simple mean would result in a static series devoid of variability, reconstruction based on regression equations allows for capturing seasonality and the alternation of precipitation events. This approach preserves the climatic characteristics of the Eastern Amazon with greater fidelity, which is essential for the integrity of the reconstructed time series.

GPM (0.22) and NP (0.19) stood out, suggesting a better ability to capture temporal variability compared to the other bases, while Xavier obtained the lowest value (0.09). Still, the relatively low magnitude of these values is consistent with studies conducted in tropical regions, where the high spatio-temporal variability of rainfall, combined with the

occurrence of intense and localized convective events, tends to compromise daily-scale fit [2, 39].

The mean bias (PBIAS) ranged from − 17% (NASA Power) to -30.0% (CHIRPS and Xavier), indicating a general trend toward underestimating daily precipitation in all analyzed datasets. The smallest bias was observed in NP (–17%), evidencing closer proximity between estimated and observed values. Conversely, INMET presented the largest deviation (–47%), suggesting a higher propensity to underestimate precipitation totals. Intermediate values were recorded for GPM (–29%), CHIRPS, and Xavier (–30%), all pointing toward a slight to moderate underestimation of rain events. Similar results have been reported by studies in humid tropical regions, where atmospheric complexity and the convective nature of rainfall favor systematic deviations in satellite-based or reanalysis products [25, 26, 30]. Despite these limitations, the relatively low PBIAS values suggest that, in general, the analyzed bases did not present extreme overestimation or underestimation trends, which is a favorable aspect for their application in time series gap-filling.

Willmott's index of agreement (d) ranged from 0.54 (Xavier) to 0.65 (GPM), reflecting moderate to high agreement between observed and estimated values across the different bases. GPM presented the highest value (0.65), suggesting better performance in reproducing the magnitude of precipitation events, although accompanied by uncertainties associated with other indicators such as RMSE and PBIAS. INMET obtained d = 0.60, while NP (0.58) and CHIRPS (0.55) showed intermediate performance, both indicating reasonable levels of correspondence with observed data. The lowest value was recorded for Xavier (0.54), though still within the range considered acceptable in comparative rainfall studies. Similar results have been reported in studies conducted in the Amazon, where the spatial heterogeneity of convective rainfall contributed to reduced agreement between estimates and observations at a daily scale [5, 10].

In general, although GPM showed better performance in the correlation coefficients (R^2, NSE, and index d), NASA POWER stood out for the lowest error values (RMSE = 10.64 mm) and bias (–17%), indicating greater statistical precision relative to the tower data. Thus, this base was considered the most suitable for filling the historical series gaps and was used to estimate the 209 missing days.

3.3 Temporal Analysis of Accumulated Precipitation

The analysis of cumulative precipitation highlights the pattern of strong seasonal variability characteristic of the Amazon region, reflected in the upward trend of the curves throughout the evaluated period (Fig. 5). It is observed that all databases presented an evolution consistent with the progressive increment of rainfall, following the pattern of increase during wet periods and relative stabilization during drier periods. This behavior demonstrates that, in general, the analyzed series adequately captured regional seasonality,

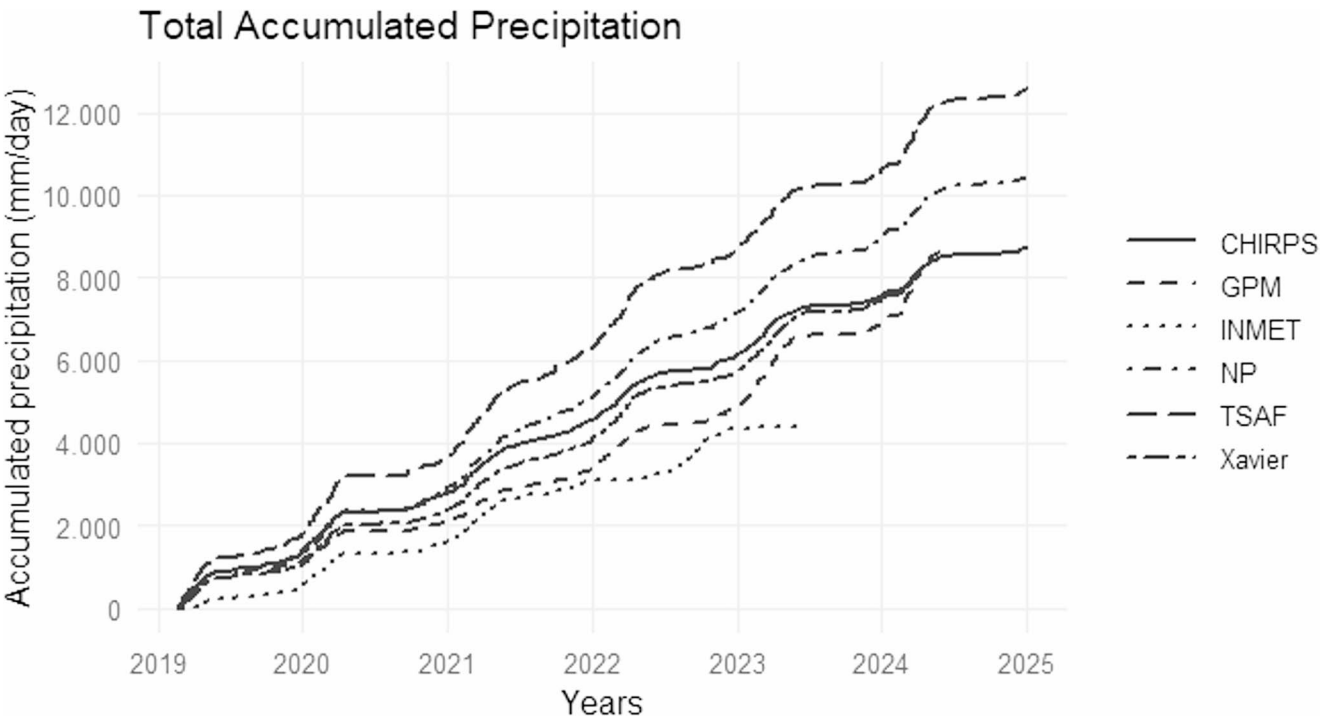

Fig. 5 Accumulated daily precipitation curve (mm/day) for the period from 2019 to 2024, comparing the observed data with the estimates from the GPM, NP, CHIRPS, INMET, and Xavier datasets

albeit with differences regarding the total accumulated volume and the intensity of the increments over the years.

The TSAF presented the highest cumulative precipitation values, showing greater sensitivity to intense rainfall events recorded locally. Among the evaluated bases, the NP product stood out for its closer proximity to the TSAF, consistently reproducing the precipitation growth trend over the period, although with slightly lower values. The CHIRPS database also showed similar behavior, following the temporal variability but with a slight underestimation of the total accumulation.

On the other hand, the Xavier, GPM, and INMET bases showed greater divergence from the TSAF, especially from the middle of the series onward, where a lower accumulation of precipitation is observed. This underestimation may be associated with limitations in the spatial resolution of satellite products and the point representativeness of conventional stations, which do not always capture the spatial heterogeneity of rainfall in the Amazon [24]. Nevertheless, these series followed the seasonal pattern of alternation between rainy and less rainy periods, which reinforces the consistency of the general behavior of the estimates [42].

Overall, the results confirm that while all analyzed bases capture the typical seasonality of precipitation in the Eastern Amazon region, there are significant differences regarding the total accumulated volume. The proximity between the TSAF and the NP and CHIRPS series suggests that these bases possess a greater capacity to represent the temporal variability of rainfall at a local scale, which is in line with the previously discussed statistical indicators. Conversely, the underestimations observed in Xavier, GPM, and INMET highlight restrictions that may compromise the direct application of these series for more detailed hydrological analyses, especially in studies requiring higher precision in the water balance. Thus, the joint evaluation of statistical indicators and cumulative rainfall behavior reinforces the choice of the NP base as the most suitable for gap-filling the TSAF series, ensuring greater data reliability.

Figure 5 presents the analysis of daily cumulative precipitation for the 2019–2024 period. Although all series show the same cumulative upward trend over time, indicating consistency in seasonality and rainfall distribution patterns, there are relative differences in the total accumulated volume between the bases.

4 Conclusion

This study evaluated the performance of satellite-based and gridded precipitation products for gap-filling daily rainfall series in an agroforestry system (AFS) in the Eastern Amazon. Our results confirm that, although all datasets capture regional seasonality, performance at the daily scale varies significantly due to the high spatio-temporal variability of tropical convective events.

The NASA POWER dataset emerged as the most reliable source for gap-filling in the Eastern Amazon, presenting the lowest overall error (RMSE = 10.64 mm) and systematic bias (PBIAS = -17.0%). Although GPM (IMERG) demonstrated a superior agreement index (d = 0.65), the stability and low PBIAS of NASA POWER consolidate it as a robust alternative for maintaining data continuity in remote tropical regions, faithfully representing seasonality and long-term trends. However, the identified systematic underestimation requires caution in high-precision applications, such as irrigation planning and crop water balance. Thus, users in areas with a scarcity of stations should consider these error limits to mitigate impacts on agricultural management, with future research being necessary to establish specific tolerance levels for these errors in different Amazonian production systems.

Despite a general trend toward underestimation across all products, the results demonstrate that satellite-derived data perform better than using the simple mean of the observed series for gap-filling. Consequently, this methodology proves essential for sustainable water resource management and hydrological modeling in agricultural production areas, such as agroforestry systems, where rain gauge networks are often sparse. Future research should incorporate seasonal evaluations and regional statistical adjustments to further refine the accuracy of these estimates during extreme climatic events.

Acknowledgements We thank the Large-Scale Biosphere-Atmosphere Program in the Amazon (LBA) for the technical, logistical, and infrastructure support during the field measurements; the landowner, Mr. Jailson Takamatsu; the partners of the SAF-Dendê Project: the Brazilian Agricultural Research Corporation (EMBRAPA), Natura Inovação e Tecnologia, the International Centre for Research in Agroforestry (ICRAF), United States Agency for International Development (USAID) and the Mixed Agricultural Cooperative of Tomé-Açu (CAMTA); the Graduate Program in Agronomy (PGAgro/UFRA); and the Coordination for the Improvement of Higher Education Personnel (CAPES) for the graduate scholarship granted to Giselle Nerino Brito de Souza.

Author contributions Giselle Nerino Brito de Souza: Conceptualization, Methodology design, Data curation, Formal analysis, Investigation, Writing – original draft preparation, Writing – review and editing, Visualization. Julie Andrews de França e Silva: Data curation, Formal analysis, Writing – review and editing. Kaleb Lima Ribeiro: Data curation, Formal analysis, Writing – review and editing.Leonardo Ramos de Oliveira: Methodology , Data curation, Visualization, Writing. Paulo Ricardo Teixeira da Silva: Software, Formal analysis, Visualization. Débora Cristina Castellani: Project administration, Resources, Writing – review and editing. Júlio Sílvio de Sousa Bueno Filho: Supervision, review and editing. Alailson Venceslau Santiago: Software, Data curation. Steel Silva Vasconcelos: Resources, Writing – review and editing. Wenceslau Geraldes Teixeira: Supervision, Resources, Writing – review and editing. Alessandro Carioca de Araújo: Funding acquisition, Supervision, Resources, Writing – review and editing.

Funding The Article Processing Charge (APC) for the publication of this research was funded by the Coordenação de Aperfeiçoamento de Pessoal de Nível Superior - Brasil (CAPES) (ROR identifier: 00x0ma614).

Data Availability The datasets generated and analyzed during this study are available upon reasonable request to the corresponding author or on the websites and directories suggested for each database. The NASA Power precipitation dataset is available at (https://power.larc.nasa.gov/data-access-viewer), the GPM precipitation dataset is available at (https://gpm.nasa.gov/data/directory), the CHIRPS precipitation dataset is available at (https://data.chc.ucsb.edu/products/CHIRPS-2.0/), the INMET precipitation dataset is available at (https://bdmep.inmet.gov.br/), the Xavier precipitation dataset is available at (https://github.com/AlexandreCandidoXavier/BR-DWGD), and the precipitation dataset from the micrometeorological observation tower located in Tomé-Açu, Pará, Brazil, is available at (https://programalba.cloud).

Declarations

Competing interests The authors declare no competing interests.

Source of financing Natura Inovação e Tecnologia; United States Agency for International Development (USAID) and the Large-Scale Biosphere-Atmosphere Programme in Amazonia (LBA) for technical, logistical and infrastructure support during the complexities of the field.

References

1. Alvares CA, Stape JL, Sentelhas PC, Moraes Gonçalves JL, Sparovek G (2013) Köppen's climate classification map for Brazil. Meteorol Z 22:711–728. https://doi.org/10.1127/0941-2948/2013/0507
2. Alves GF, de Victoria D C (2020) Avaliação da precipitação estimada pelo GPM Late Run para estações meteorológicas no Brasil. Portal Embrapa. Embrapa Agricultura Digit, p. 1–8
3. Barros PC, Costa ANM, Gomes MF et al (2025) Floristic composition and temporal dynamics of oil palm agroforests in the eastern Amazon. Agroforest Syst 99:86. https://doi.org/10.1007/s10457-025-01175-y
4. Berenguer E et al (2021) Tracking the impacts of El Niño drought and fire in human-modified Amazonian forests. Proc Natl Acad Sci USA 118:30. https://doi.org/10.1073/pnas.2019377118
5. Bezerra D, de Silva Júnior F, Gonçalves JC, G. E., de Medeiros E, V. W. C (2019) Availability analysis of the Brazilian's national weather measurement system. Revista Brasileira de Computação Aplicada 11:3, 146–154. https://doi.org/10.5335/rbca.v11i3.10026
6. Campbell Scientific, Inc (2018) Instruction Manual: TE525 Tipping Bucket Rain Gage. Logan, Utah: Campbell Scientific. Disponível em: https://s.campbellsci.com/documents/br/manuals/te525.pdf. Acesso em: 10 abr. 2025
7. CEMADEN – Centro Nacional de Monitoramento e Alertas de Desastres Naturais Procedimento de limpeza do pluviômetro. Cachoeira Paulista: CEMADEN, [s.d.]. Folheto institucional
8. Chen M et al (2017) Assessment of satellite precipitation products in South America. J Hydrometeorol 18(2):529–546
9. D'Almeida C, Vörösmarty CJ, Hurtt GC, Marengo JA, Dingman SL, Keim BD (2007) The effects of deforestation on the hydrological cycle in Amazonia: a review on scale and resolution. Int J Climatol 27:633–647. https://doi.org/10.1002/joc.1475
10. De Moraes Cordeiro AL, Blanco CJC (2021) Assessment of satellite products for filling rainfall data gaps in the Amazon region. *Natural Resource Modeling*, v. 34, n. 2, p. e 12298
11. Espinoza JC et al (2014) The role of the South American Monsoon System in the intensification of the Amazonian droughts. Clim Dyn 43:337–353. https://doi.org/10.1007/s00382-013-1832-0
12. FUNDAÇÃO GETÚLIO VARGAS (2020) Diagnóstico e Proposição de Bases Climáticas para o Brasil. FGV Energia, Rio de Janeiro
13. Funk C, Peterson P, Landsfeld M, Pedreros D, Verdin J, Shukla S, Michaelsen J (2015) The climate hazards infrared precipitation with stations - A new environmental record for monitoring extremes. Sci Data 2:150066. https://doi.org/10.1038/sdata.2015.66
14. Huffman GJ, Bolvin DT, Braithwaite D, Hsu K, Joyce R, Kidd C, Xie P (2019) Integrated Multi-satellite Retrievals for the Global Precipitation Measurement (GPM) Mission (IMERG), Version 6. *NASA's Precipitation Processing Center*. https://doi.org/10.5067/GPM/IMERG/3B-HH/06
15. INMET – Instituto Nacional de Meteorologia. Manual de instalação, operação e manutenção de estações meteorológicas automáticas (2008) Brasília: INMET. Disponível em: https://portal.inmet.gov.br/manual/manual_estacoes_automaticas.pdf. Acesso em: 10 abr. 2025
16. INMET – Instituto Nacional de Meteorologia (2023) Banco de Dados Meteorológicos para Ensino e Pesquisa. Disponível em: https://bdmep.inmet.gov.br/
17. Jiménez- Muñoz JC et al (2016) Record-breaking warming and extreme drought in the Amazon rainforest during the course of El Niño 2015–2016. Sci Rep 6:33130. https://doi.org/10.1038/srep33130
18. Legg TP et al (2021) Evaluation of remote sensing rainfall products for hydrological modeling in the Amazon basin. Hydrol Earth Syst Sci 25:1–21
19. Leite-Filho AT, Soares-Filho BS, Davis JL, Abrahão GM, Borner J (2021) Deforestation reduces rainfall and agricultural revenues in the Brazilian Amazon. Nat Commun 12(1). https://doi.org/10.1038/s41467-021-22840-7
20. Lentini M et al (2021) Agricultura familiar resiliente: aprendizados de 20 anos de sistemas agroflorestais no Pará. Imazon, Belém, p 80
21. Marengo JA, Espinoza JC (2016) Extreme Seasonal Droughts and Floods in Amazonia: Causes, Trends and Impacts. Int J Climatol 36:1033–1050. https://doi.org/10.1002/joc.4420
22. Marengo JA et al (2020) A qualidade dos dados de precipitação no Brasil: comparação entre dados de reanálise, satélite e observações in situ. Revista Brasileira de Meteorologia 35(3):377–390. https://doi.org/10.1590/0102-778635320190063
23. Marengo J, Cunha A, Espinoza J, Fu R, Schöngart J, Jimenez J, Costa M, Ribeiro J, Wongchuig S, Zhao S (2024) The Drought of Amazonia in 2023–2024. Am J Clim Change 13:567–597. https://doi.org/10.4236/ajcc.2024.133026
24. Meira MA, Freitas ES, Coelho VHR, Tomasella J, Fowler HJ, Ramos Filho GM, Silva AL, Almeida C, das N (2022) Quality control procedures for sub-hourly rainfall data: An investigation in different spatio-temporal scales in Brazil. J Hydrol 613. https://doi.org/10.1016/j.jhydrol.2022.128358. Part A

25. Monteiro JEBA, Sentelhas PC, Pedra MAG (2018) Desempenho do banco de dados meteorológicos da NASA POWER para aplicação em modelos agroclimáticos no Brasil. Revista Brasileira de Engenharia Agrícola e Ambiental 22(10):679–685. https://doi.org/10.1590/1807-1929/agriambi.v22n10p679-685
26. Monteiro JEBA et al (2021) Comparação de produtos de precipitação via satélite com dados observacionais em diferentes biomas do Brasil. Revista Brasileira de Climatologia 28:1–20. https://doi.org/10.5380/abclima.v28i0.75938
27. Moriasi DN et al (2007) Model evaluation guidelines for systematic quantification of accuracy in watershed simulations. Trans ASABE 50:885–900. https://doi.org/10.13031/2013.23153
28. NASA POWER (2021) Prediction Of Worldwide Energy Resources. Disponível em: https://power.larc.nasa.gov/
29. Paiva RCD et al (2011) Rainfall-Runoff Modelling in the Amazon Basin Using the MGB-IPH Model. Hydrol Sci J 56(5):799–817
30. Paredes-Trejo FJ, Barbosa HA, Lakshmi Kumar TV (2017) Validating Chirps - Based Satellite Precipitation Estimates in Northeast Brazil. J Arid Environ 139:26–40. https://doi.org/10.1016/j.jaridenv.2016.12.009
31. Pereira Filho AJ et al (2018) Climate and Weather of the Amazon. Amazônia: recursos naturais e sociedade. Oficina de Textos, São Paulo, pp 45–78
32. Rodrigues TE, Santos PL, Rollim PAM, Santos E, Rego RS, Silva JML, Gama JRN (2001) Caracterização e classificação dos solos do Município de Tomé Açu, PA. Embrapa Amazônia Oriental, Belém, Documento 117
33. Santos CAG, Silva RM, Souza WJ (2016) Uso de sensores para o monitoramento de variáveis hidroambientais. *Revista Brasileira de Recursos Hídricos*, Porto Alegre, v. 21, n. 1, pp. 38–49
34. Schaefli B, Gupta H (2007) Do Nash values have value? Hydrol Process 21(15):2075–2080. https://doi.org/10.1002/hyp.6825
35. Shi H et al (2022) Using isotopic partitioning of evapotranspiration to improve hydrological modeling: a HYDRUS-1D study. J Hydrol 610:127947. https://doi.org/10.1016/j.jhydrol.2022.127947
36. Silva FR, da et al (2022) Preenchimento de falhas em séries temporais de precipitação: comparação de métodos e impactos em simulações hidrológicas. Revista Brasileira de Recursos Hídricos, v. 27
37. de Souza EB et al (2012) Padrões espaço-temporal pluviométricos na Amazônia Oriental utilizando análise multivariada. Revista Brasileira de Meteorologia 401–412 São Paulo, v. 27, n. 4. https://doi.org/10.1590/S0102-77862012000400006
38. Stackhouse PPD Jr (2020) NASA POWER. Prediction Of Worldwide Energy Resources. Methodology. 2020. Disponível em: https://power.larc.nasa.gov/docs/methodology/
39. Tan J et al (2017) Performance of IMERG as a function of spatiotemporal scale. *Journal of Hydrometeorology*, Boston, v. 18, n. 2, pp. 307–319. https://doi.org/10.1175/JHM-D-16-0174.1
40. Tomasella J, Hodnett MG, Cuartas LA, Nobre AD, Waterloo MJ, Oliveira S (2008) The water balance of an Amazonian micro-catchment: the effect of interannual variability of rainfall on hydrological behavior. Hydrogeological Processes 22:2133–2147. https://doi.org/10.1002/hyp.6813
41. Towner J, Ficchí A, Cloke HL, Bazo J, Coughlan de Perez E, Stephens EM (2021) Influence of ENSO and Tropical Atlantic Climate Variability on Flood Characteristics in the Amazon Basin. Hydrol Earth Syst Sci 25:3875–3895. https://doi.org/10.5194/hess-25-3875-2021
42. Turco JEP, Carleto N (2017) INTEGRIDADE DE DADOS METEOROLÓGICOS PARA USO EM MODELO HIDROLÓGICOMETEOROLÓGICOS PARA USO EM MODELO HIDROLÓGICO. Revista Brasileira De Agricultura Irrigada 11(8):2084–2097. https://doi.org/10.7127/rbai.v11n800668
43. Willmott CJ, Robeson SM, Mako MJ (2012) Statistics for the evaluation and comparison of models. In: BENSON J (ed) Modeling environmental change. Springer, Berlin, pp 35–56. https://doi.org/10.1007/978-3-642-22405-4_3
44. Xavier AC, King CW, Scalon BR (2016) Daily gridded meteorological variables in Brazil (1980–2013). Int J Climatol 36(6):2644–2659
45. Yoon JH, Zeng N (2010) An Atlantic influence on Amazon rainfall. Clim Dyn 34:249–264
46. Zambrano-Bigiarini M, Rivas M (2020) H*ydroGOF: Goodness-of-fit functions for comparison of simulated and observed hydrological time series*. R package version 0.4-0
47. Zandonadi L et al (2022) Avaliação do desempenho de produtos satelitais de precipitação na Amazônia Oriental. *Boletim de Ciências Geodésicas*, v. 28, n. 1. https://doi.org/10.1590/bcg.v28i1.2391
48. Zárate-Salazar JR et al (2024) First approximation of soil quality critical limits in land use systems in the Brazilian Amazon. *CATENA*, 247. https://doi.org/10.1016/j.catena.2024.108476